Title: Light sheet fluorescence microscopy for neuroscience

Author: Stella Corsetti Frank Gunn-Moore Kishan Dholakia

PII: S0165-0270(18)30218-8
DOI: https://doi.org/doi:10.1016/j.jneumeth.2018.07.011
Reference: NSM 8062

To appear in: *Journal of Neuroscience Methods*

Received date: 12-4-2018
Revised date: 3-6-2018
Accepted date: 16-7-2018

Please cite this article as: Stella Corsetti, Frank Gunn-Moore, Kishan Dholakia, Light sheet fluorescence microscopy for neuroscience, *<![CDATA[Journal of Neuroscience Methods]]>* (2018), https://doi.org/10.1016/j.jneumeth.2018.07.011

Light sheet fluorescence microscopy for neuroscience

Stella Corsetti[a,*], Frank Gunn-Moore[b], Kishan Dholakia[a,*]

[a] *Scottish Universities Physics Alliance, School of Physics and Astronomy, University of St. Andrews, North Haugh, St. Andrews, Fife KY16 9SS, UK.*
[b] *School of Biology, University of St. Andrews, North Haugh, St. Andrews, Fife KY16 9ST, UK.*

Abstract

Background

The functions of the central nervous system (CNS) rely on the interaction between large populations of neurons across different areas. Therefore, to comprehend CNS functions there is a need for imaging techniques providing access to the neuronal activity of large networks of neurons with very high spatiotemporal resolution.

New method

Light sheet fluorescence microscopy (LSFM) is a very promising optical sectioning technique that allows volumetric imaging over many length scales while retaining high spatial resolution and minimizing photobleaching and phototoxicity.

Results

The application of LSFM in neuroscience opened up the possibility of imaging *in-vivo* the development of the CNS and acquiring morphological images of whole cleared mammalian brains with sub-cellular resolution. The use of propagation invariant Bessel and Airy beams has shown potential for increasing the penetration depth in turbid neural tissues.

Comparison with existing methods

The lack of temporal and/or spatial resolution of traditional neuroscience imag-

*Corresponding author
Email addresses: sc337@st-andrews.ac.uk (Stella Corsetti), kd1@st-andrews.ac.uk (Kishan Dholakia)

ing techniques call attention to a need for a technique capable of providing high spatio temporal resolution. LSFM, which is capable of acquiring high resolution volumetric images is increasingly becoming an interesting imaging technique for neuroscience.

Conclusions

The use of different LSFM geometries has shown the potential of this technique in acquiring *in-vivo* functional images of the CNS and morphological images of entire cleared mammalian brains. Further development of single objective LSFM implementations and fibre based LSFM combined with the use of propagation invariant beams could allow this technique to be used for in depth *in-vivo* imaging.

Keywords: Light sheet fluorescence microscopy, LSFM, Neuroimaging, Neuroscience, SPIM, Airy beams, Bessel beams, brain.

1. Introduction

The development, maturation and maintenance of the nervous system, its anatomical and functional structure, with particular attention to the brain and the role it plays in behavior and cognition, has been the centre of much scientific investigation. The functional unit of the nervous system is the neuron which integrates external inputs and sends out signals to other regions which ultimately guides behavior. The neuron consists of a cellular body (soma), dendrites and an axon. Dendrites are thin tree-like extensions that branch off the soma and can extend for hundreds of micrometres. The axon is a cellular extension that arises from the soma and can transmit information from micrometres to a metre in the human body. Groups of neurons are organized into complex three-dimensional circuits containing tens of different cellular subtypes arranged in specialized functional sub-networks. The brain's diverse functions rely on the interaction between large populations of neurons across different areas of the brain. Signals are received by the soma and the dendrites. These signals are then sent to other neurons in a time frame of a few milliseconds via the axon to specific structures

referred to as dendritic spines or synapses.

Neuroscientists seek to understand not only the normal mechanisms of the nervous system, but also the nature of developmental and neurological disorders with the intent of finding new ways to prevent or treat them. In order to obtain this knowledge, it is necessary to unveil how sensory information is processed by neuronal networks and how a behavioral output is produced. The models systems utilised are diverse ranging from using larval and adult zebrafish, invertebrate model species, such as Drosophila melanogaster and Caenorhabditis elegans, and also rodent mammals. In order to be useful as an animal model, the organism should be able to exhibit physiological, pathological or behavioral features of the human disease. However, with regards to imaging, the choice of the most appropriate animal model is not always based on the one that is best suited to address a specific question of interest. For example, larval zebrafish are a poor anatomical model for the human brain but they are frequently used because they are transparent and therefore easy to be imaged. Drosophila and C. elegans have also been used as models for brain diseases because they offer advantages in terms of a high degree of genetical control and they also have a relatively short lifetime; however, they are far removed phylogenetically from mammals. Among mammals, mice are by far the species most used to gain insights into the pathogenesis of neurodegeneration (e.g. Alzheimers disease) even if they cannot be affected normally by this pathology [1]. Despite this, the main reason for their use relies on again the ability to control their genetic make-up but also the relatively small size of their brain which again makes it easier to be imaged. However, irrespective of the model, there is a need for imaging techniques to provide a full spatio-temporal access to the neuronal activity of large networks of neurons but with sub-cellular and millisecond resolution [2, 3].

1.1. Why should we use optical imaging in neuroscience?

Optical imaging has advantages over traditional neuroscience imaging techniques such as Electroencephalography (EEG), Magnetoencephalography (MEG), functional Magnetic Resonance Imaging (fMRI) and Positron Emission Tomog-

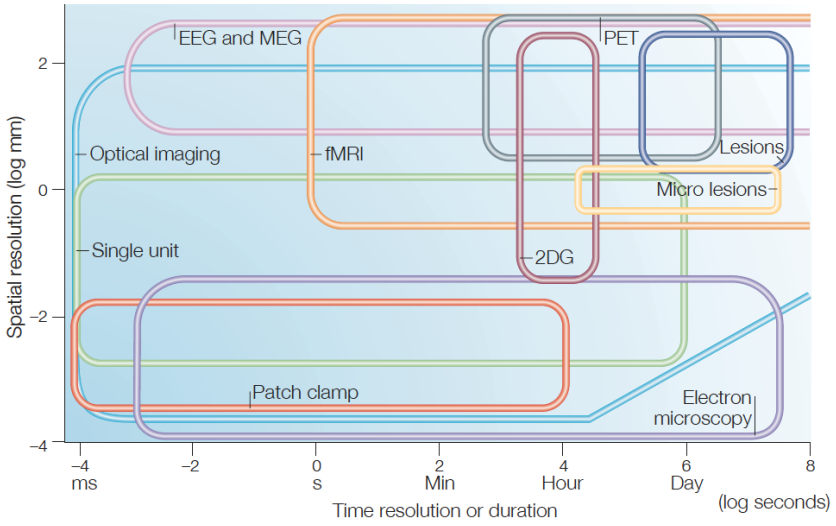

Figure 1: Imaging techniques used in neuroscience. The coloured rectangles represent the spatiotemporal capabilities of each technique. Notice, optical imaging covers almost the entire area occupied by the others techniques. Image reproduced with permission from [4].

raphy (PET). A major advantage is the potential optical imaging of the nervous system over many length scales: from the single synapse to the entire brain, while retaining the capability of achieving very high spatio-temporal resolution (see Figure 1).

The latter capability is a necessary requisite if fast events such as action potentials are to be resolved. Their flexibility and easiness to be modified makes optical setups suitable to be integrated with many other techniques for multi modal imaging. Another advantage is the possibility of selectively labeling different neurons and recording their activity as changes in optical brightness, by using engineered light-emitting protein sensors, termed genetically encoded voltage indicators (GEVis). GEVis relate changes in voltage to changes in brightness by sensing the neuron membrane potential. Also neuroscientists have relied on encoded calcium indicators (GECIs) in order to follow rapid post-synaptic events. GECIs are florescent proteins modified so that their folding properties are sensitive to the calcium concentration that changes within the cell after the

firing of an action potential. Therefore, local changes in calcium concentration can be used as an indirect measure of voltage transients in neurons. However, the kinetics of calcium transients is relatively slow and GEVis need to be used in order to report sub-threshold electrical activity in dendritic and somatic membranes, though the speed of activity means that its recording usually requires specialised optics.

The development of confocal microscopy was a key initial step to enable optical imaging for neuroscience research. Confocal microscopy uses an epifluorescence geometry, in which the objective lens used to send the excitation light to the sample is the same used to collect the emitted fluorescence. In confocal microscopy the out of plane unfocused light is rejected by using a spatial pinhole; however, the optical sectioning is not obtained in the illumination process, therefore, as in wide field microscopy, the specimen is subjected to wide light exposure. Furthermore, the sample is scanned one point at a time rendering the acquisition of volumetric images very long. The wide light exposure combined with the limited acquisition speed results in a much higher exposure of the sample causing potential photobleaching. Moreover, high resolution imaging deep into biological tissues is not possible. Deeper penetration and a lower attenuation can be achieved by using two-photon microscopy (2PM) in an analogous geometry, which has been employed to visualise neuronal activity both at the single synapse level [5, 6, 7] and at the whole brain level [8, 9, 10]. In 2PM a fluorophore is excited to a higher state, by absorbing two photons with combined energies similar to that which is needed to excite the fluorophore to the same state using a single photon. The use of longer infrared wavelengths (650 nm to 1200 nm) reduces autofluorescence and absorption by biological samples. 2PM provides both high lateral and axial resolution and high sensitivity inside scattering tissues [11], while reducing photobleaching by exciting only a single point in space. However, single point scanning 2PM has a limited temporal resolution due to the fact that three dimensional imaging cannot be achieved by scanning a single point trough a 3D volume. A minimum laser dwell time of the order of 1 sec is needed to collect a significant number of photons in a

given voxel [12] limiting the acquisition rate to $\sim 10^6$ voxels per second. This drastic limit imposed by single scanning point techniques, limits the number of neurons that can be dynamically recorded making these approaches limiting for imaging in neuroscience. In order to improve parallelization, other implementations such as simultaneous multi-point excitation [13, 14, 15], and temporal focusing [8, 16, 17, 18] can be considered. However, these methods add both experimental complexity and cost. Random-access imaging including acousto-optical deflectors [19, 20, 21, 22], has been used to rapidly record the activity of multiple neurons in the intact brain [21]. However, this approach samples the volume sparsely at different points and is highly sensitive to motion, and so cannot be used in freely moving organisms [22, 23]. Sub-diffraction resolution down to a few tens of nanometers can be achieved by using super resolution techniques such as stimulated emission depletion (STED) microscopy, photo-activated localization microscopy (PALM) or stochastic optical reconstruction microscopy (STORM) but at the expense of both penetration depth (a few microns at most) and speed. While PALM and STORM are based on single molecule switching and localization, STED additionally allows the individual identification of molecules at high densities and the analysis of their distributions and dynamics using patterned illumination. However, an important aspect to be taken into account when considering optical imaging techniques is that resolution, penetration depth and speed are competing parameters. In STED the imaging speed is typically lower than for confocal or 2P microscopy, due to the longer pixel dwell-time which is necessary to collect more photons from a smaller region. Furthermore, as with any other light microscopy techniques, penetration depth is limited by scattering. STED has been used to visualise dendritic spine shapes in living neurons with exceptional resolution [24]. Due to their single molecule nature PALM and STORM are capable of achieving a lateral spatial resolution of 10-30 nm. Advances in image processing algorithms have rendered possible the use of PALM and STORM to image living cells reducing acquisition times for 2D images down to a few seconds [25, 26]. However, being based on wide field illumination, both techniques have very lim-

ited penetration depth. PALM and STORM have been mainly used to study postsynaptic receptors and scaffold proteins [27, 28, 29].

An optical imaging technique with high temporal resolution which is limited only by the camera and photon count, is light field microscopy (LFM) [30, 31]. In this technique, the sensor pixels capture the light field rays coming from a microlens array placed in the native image plane. In this way, 4D light field information from both a 2D location and a 2D angle of the incident light, is captured via a single sensor image without the need for scanning. High speed volumetric acquisition is enabled by computationally reconstructing the full 3D volume from the recorded light field in single sensor images. Prevedel et al [32] imaged the simultaneous functional imaging of neuronal activity in an entire C. elegans and larval zebrafish brain using LFM in combination with a 3D deconvolution algorithm improving the technique spatial resolution. Nevertheless, LFM is still limited in spatial resolution when compared to 2PM.

However, while all of these techniques are very exciting from an optical viewpoint, many have yet to find a dominant role in neuroscience research due to shortenings including the inability to image over large scales and photodamaging effects.

1.2. Light sheet fluorescence microscopy for neuroscience: where we are and what do we need

A technique that allows us to navigate flexibly between resolution, penetration depth and acquisition speed while minimizing photodamage, is light sheet fluorescence microscopy (LSFM). LSFM is an optical sectioning technique capable of retaining high spatial resolution while performing volumetric imaging. In contrast to single point scanning techniques, it excites the tissue locally with a thin sheet of light instead of using a focused spot. This allows the acquisition speed of volumetric images to be increased by one-to-two orders of magnitude [33, 34, 35] while minimizing photobleaching and phototoxicity [36, 37, 38, 39]. In LSFM the fluorescence is excited with a light sheet only around the focal plane of the detection objective which is oriented perpendicular to the illumi-

nation axis. Moreover, a 3D stack of images is acquired illuminating each plane only once. The combination of these characteristics leads to a reduction of the energy load on the specimen reducing phototoxic effects [40]. LSFM enables volumetric imaging while avoiding exposure of the sample to light beyond the focal plane resulting in the gentlest fluorescence microscopy technique available to date [40, 41, 42]. A few studies on developmental biology comparing photobleaching and phototoxicity between confocal and LSFM setups have been conducted [38, 39]. J. Icha et al [39] compared a published dataset of cell cycle phase lengths of zebrafish retinal neuronal progenitors acquired in several confocal setups [43] with data acquired in LSFM. They observed a prolonged cell cycle phase's length in the confocal dataset due to phototoxicity. Wu Y et al. [44] imaged C. elegans embryogenesis with a LSFM setup at 30 times higher time resolution compared to a spinning disk confocal setup due to the lower phototoxicity [39]. A reduction in photobleaching and photoxicity by up to three orders of magnitude has been reported when using LSFM instead of confocal microscopy [40]. The lower photodamage effects make this technique particularly suited for developmental biology studies [44, 45], for imaging large fixed specimens, such as mammalian brains [46, 47], and for *in-vivo* studies [34, 48, 49, 50].

However, it is important to understand the current capabilities of LSFM for neuroscience and what we need to achieve in future. Presently we are capable of imaging *in-vivo* processes with sub-cellular resolution at very high speeds ($\sim$ 100 Hz) but with limited penetration depth ($\sim$ 20-100 μm)[51]. We are also capable of recording spatially isotropic whole brain functional images in larval zebrafishes at 1 Hz with sub-cellular resolution [34]. However, what researchers really need is to acquire functional images from a large population of neurons at 10-20 ms resolution, in order to resolve single spikes. Therefore, much higher acquisition speeds over large volumes is required. Furthermore, we need to image not only transparent samples, such as larval zebrafishes, but also non-transparent brain structures that extend over considerable volumes as is the case for mammalian brains. This requires fast volumetric techniques capable

of imaging deep into turbid tissues. However, one of the main challenges when imaging in depth with high resolution is posed by the high absorption and strong scattering.

One strategy to circumvent this problem and obtain enhanced imaging is rendering tissues transparent by using optical clearing techniques. The basic principal of optical clearing is to achieve uniformness of the refractive index of biological samples. This can be obtained by penetrating optical clearing agents which have a high refractive index into the extracellular space in order to match the high refractive index of cells, collagen and elastic fibres [52, 53, 54], or by removing lipids, which are the main source of scattering in tissues [54]. Thanks to the use of these methods, we can now image small mammalian brains with sub cellular resolution [47]. A more in depth discussion about optical clearing methods and their use in imaging mammalian brains with LSFM will be given in section 3.2. These methods are useful to image fixed samples, but in order to image brains *in-vivo* other solutions need to be found. One possibility is using 2P LSFM in which the use of longer wavelengths and the fact that fluorescence is proportional to the square of the intensity, makes imaging less susceptible to degradation by out of focus absorption and scattering. At the moment by using 1P (single photon) LSFM, we are capable of imaging superficial layers of the brain of an awake mouse at 20 Hz with the possibility of resolving 5-10 μm in size single capillaries at a depth of 140 μm [50]. Deeper penetration depth would be achieved by using 2P LSFM. However, even bigger extension of the depth-of-field can be achieved by using non-diffractive beams instead of Gaussian beams. This latter aspect will be discussed in section 2.2. Substantially, what we really need is increased acquisition speed, high resolution and deeper penetration depth in non-transparent samples at the same time.

2. Light sheet fluorescence microscopy

Even though the geometry for optical sectioning used in LSFM was first shown in 1902 [55], the possibility of using light sheet for biological studies

was recognised only in 2004 [12]. In LSFM two distinct orthogonal optical paths are combined, one for illumination with a thin sheet of light and one for fluorescence detection. The sample is placed at the intersection between them (see Figure 2;[12]). To date most LSFM setups are built in such a way that the illumination and detection objectives lie in a horizontal plane. This geometry allows more freedom than confocal microscopy in the mounting of the organisms used as animal models in neuroscience we mentioned before. The sample can be placed in a liquid filled specimen chamber. In case of large specimens, such as mouse brains, they can be hooked by using a clip or tweezers. However, mechanical contact could induce damages to the sample therefore, the most common sample preparation technique is embedding the specimen in agarose. This method has been extensively used to image the development of different species inclusing D. melanogaster [56], C.elegans, and zebrafishes [12, 56]. **In order to ensure both immobility and growth of the embryo the sample can be mounted in low concentrations of agarose in refractive-index-matched fluorinated ethylene propylene (FEP) tubes which ensure optimal image quality from all sides [57, 58, 59].** However, one limitation of embedding samples in agarose is the possibility of restricting their movements and this is a problem when imaging developing samples. Therefore, the sample can also be placed in a container made from agarose or by using polymers and kept in position by using clips. However, it is difficult to make small agarose or polymeric chambers with thin enough walls to image the sample through them. Moreover, samples can also be imaged flat on a glass coverslip by placing the two objectives on a vertical plane. Different LSFM geometries developed to image different samples will be discussed in more detail in the next section. In LSFM different planes of the sample are illuminated, creating a z stack of images that can be 3D reconstructed, by scanning the light sheet through the sample, or by moving the sample through the focal plane. Good sectioning of the sample and out of focus light suppression is achieved by tailoring the light sheet to the micron range. In LSFM, the illumination and detection paths are decoupled and so can be optimised separately. The axial resolution is dictated both by

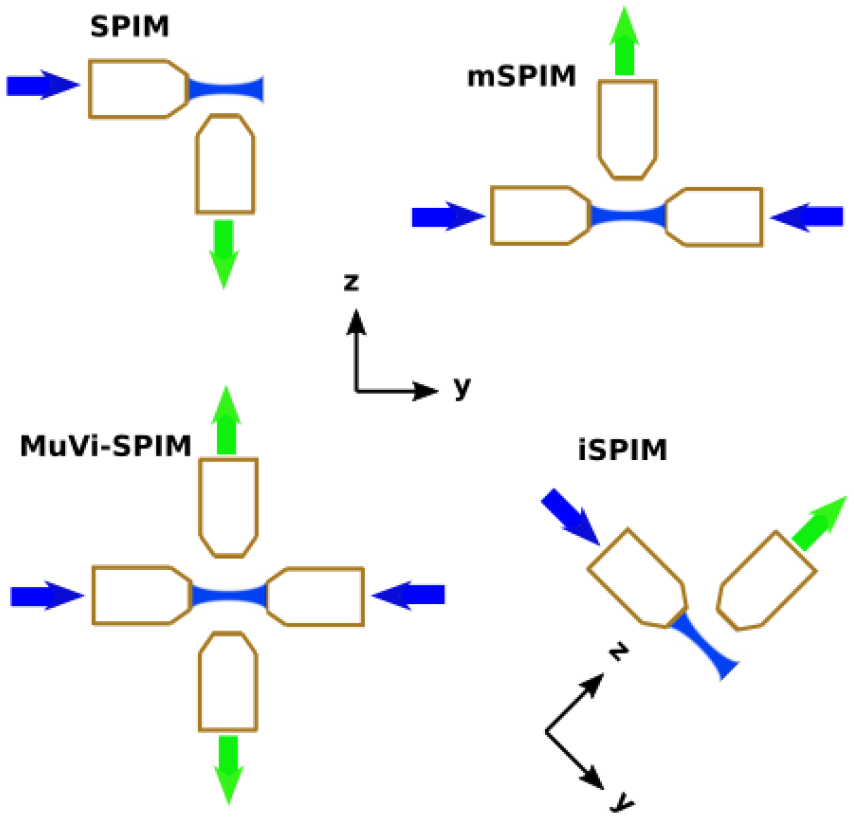

Figure 2: Schematic of standard light sheet fluorescence microscopy (LSFM) configurations.

the thickness of the sheet of light and by the numerical aperture (NA) of the detection objective. The lateral resolution is dictated solely by the NA of the detection objective and therefore, it is the same as for any widefield fluorescence microscope. In the past few years different implementations of LSFM have been developed to improve resolution imaging speed, field of view and penetration depth. Below we describe some of the most relevant LSFM implementations developed for applications in neuroscience.

2.1. Different LSFM geometries

The thin sheet of light used in LSFM can be generated by using a cylindrical lens, as in selective plane illumination microscopy (SPIM) [12] or by using a scanning mirror to rapidly scan the beam through the sample, as in digitally scanned light-sheet microscopy (DSLM) [60]. The presence of the scanning mirror offers an increased flexibility of DSLM over SPIM. The height of the light sheet can be adjusted by changing the scanning amplitude, while its thickness is related to the diameter of the incoming beam on the mirror. The formed light sheet is homogeneous leading to a uniform power density across the field of view and the penetration depth can be highly increased by using techniques such as beam shaping [61] and 2P excitation [62]. Due to the rapid scanning of the light sheet DSLM, images are less prone to striping artifacts resulting from absorption in the sample plane and though artifacts can be reduced by using propagation invariant beams [63]. On the other hand, a cylindrical lens is easy to integrate and allows the entire field of view to be illuminated simultaneously leading to a lower power per line and to an increased acquisition speed limited only by the frame rate of the camera and not by the speed of the scanning mirror.

A variant of SPIM is multidirectional SPIM (mSPIM) in which a second illumination arm, identical to the first one, illuminates the sample from the opposite direction. The images obtained from illuminating each side can be stitched together resulting in a final image of higher quality. A more even illumination and the efficient elimination of shadows can be achieved if the light sheet is resonantly pivoted about its focus [64]. The choice between the SPIM and DSLM configuration is based on the sample under investigation in order to balance photodamage effects, image quality and acquisition speed. These light sheet microscopes are set up in an horizontal plane to achieve an orthogonal configuration between the two beam paths. This geometry allows the sample to be placed at the intersection of the two paths being free to rotate in order to optimise its orientation. In SPIM the sample is moved in steps of a few microns and images are acquired in rapid succession obtaining a 3D image stack of the entire

sample volume. **In order to image deeper into the tissue the specimen can be rotated to acquire datasets from multiple angles and fuse them together into a single, high quality three-dimensional image. The sample is imaged along multiple directions, which yields improved images by collecting additional data from more favorable angles and more isotropic resolution by computationally fusing multiple sample views [56]. Each individual view is limited by low resolution along a different dimension and high resolution images in all directions can be obtained by combining different views with multiview deconvolution. However, multidirectional imaging by specimen rotation suffers from drawbacks, one of which is the difficulty of determining precisely the position and orientation of the axis of rotation relative to the specimen. Furthermore, an improved axial resolution is obtained at the expense of a reduced lateral resolution unless many volumetric views are acquired. This leads to an increased dose of radiation on the sample mitigating the original advantage of LSFM. In addition, the volumetric acquisition speed is linked to the use of ultrafast rotation stages and this limits the biological dynamics that can be visualized as well as being harmful for some biological samples. Therefore, multidirectional imaging by specimen rotation is suitable for fixed specimens, but typically not for fast processes in live specimens. By using two illumination and two detection objective lenses that are focused onto the sample from four different directions along two perpendicular axes, as in MuVi-SPIM and SIMView SPIM, it is possible to fuse images in real time and record 3D datasets without sample rotation [65, 66]. However, in order to have fully isotropic resolution at least one rotation of the specimen is needed. Both MuVi-SPIM and SIMView SPIM overcomes multidirectional imaging by specimen rotation limitations rendering possible to capture *in-vivo* imaging of fast dynamic events, such as the cellular dynamics in the early stages of CNS development of Drosophila melanogaster embryos. The**

same approach has been used in IsoView microscopy [67] in which simultaneous four-view imaging allowed spatially isotropic whole-brain functional imaging of larval zebrafish at 1Hz. IsoView microscopy improved spatial resolution and resolution isotropy of sevenfold and threefold, respectively, with respect to multidirectional imaging by specimen rotation without scaling down the acquisition volume [67]. Another system that shares these capabilities is the four-lenses selective plane illumination microscope setup development by Schmid et al. [68], which enabled the recording of the development of multiple embryos in parallel and the mapping of all labelled cells for each embryo in less than 10s.

While the horizontal configuration is more convenient for samples requiring rotation, a vertical arrangement is more suited if the sample demands a horizontal orientation. In this case the sample, usually tissue sections, is mounted on a flat surface, such as a glass slide. The vertical configuration is called inverted selective plane illumination microscopy (iSPIM) and was developed by Wu et al [44] to monitor the development of the neuronal system in C. elegans embryos with close to isotropic resolution. In this configuration, the detection and collection paths are still orthogonal to each other but are placed at a 45 degree angle relative to the sample that is usually placed on a regular microscope slide. The require for orthogonality precludes the use of the highest NA objectives which restrict space, however, if the light sheet is made sufficiently thin, the axial resolution can be decoupled from the detection NA, enabling more isotropic resolution. This configuration has been used in a compact LSFM, based on openSPIM [69], for imaging a 300 x 300 μm area of sub-neuronal structures in mammalian brain slides with a speed as high as 100 Hz [70].

An inverted configuration, termed dual-view plane illumination microscopy (diSPIM) [71], rapidly alternates excitation and detection between two identical perpendicular objectives. In diSPIM complementary views of the sample with different orientation of the point spread function are acquired improving axial resolution. An isotropic

resolution of 330 nm in imaging neuronal wiring during C. elegans brain development was achieved by using diSPIM combined with a deconvolution algorithm [71]. This method proved to be effective in imaging volumes of small transparent samples up to 80 x 80 x 50 μm^3. However, detection of larger less transparent samples requires acquisition with four-lenses LSFM configurations.

Using the above mentioned LSFM implementations volumetric data can be acquired by either moving the illumination and detection objectives synchronously to scan a stationary specimen or by moving the sample and scanning it through stationary objectives, thus limiting the imaging acquisition speed.

Different approaches have been exploited to overcome this limitation. Fahrbach et al [72] for example introduced an electrically tunable lens in the detection path to move the focal plane of the detection objective avoiding any physical movement. Increased in acquisition speed is achieved by synchronizing the frequency of the galvo mirror scanning the light sheet through the sample and the frequency of the tunable lens so that the image is always on focus on the camera. **The acquisition speed can also be increased by applying the concept of a depth of field for the imaging arm, which in LSFM was first proposed by Olarte et al. [73].** Tomer et al. [48] developed Spherical-aberration-assisted Extended Depth-of-field (SPED) LSFM which extended the depth of field by orders of magnitude, while maintaining high spatial resolution. This is achieved by introducing a thick block of altered refractive index material in the detection path of a standard LSFM inducing a spherical aberration that results in PSF elongation imaging. Using this approach they imaged the zebrafish CNS including the fully extended spinal cord in a single field of view at 6 Hz and the entire brain at 12 Hz. They also achieved sub-cellular resolution when imaging mouse brains at 1 mm depth.

However, these techniques still require the presence of two objectives rendering it difficult for their translation to in-vivo imaging. Expanding upon on the idea of the single objective light sheet setup originally suggested by Dunsby [74], Bouchard et al. [50] developed confocally-aligned planar excitation (SCAPE)

microscopy in which optically sectioned 3D data are acquired by using a single objective without the need for either the objective, or the sample, to be moved. **In SCAPE, the light sheet is swept back and forth through the sample by using an oscillating polygonal scanning mirror. The fluorescence emitted from the illuminated plane is collected by the same objective lens used for the illumination and is reflected off an adjacent facet of the scanning mirror which de-scans the light so that a stationary oblique image plane always co-aligned with the moving light sheet is formed. As this does not require any movement beyond that of one of the scanning mirrors, the speed of this technique, as in SPED, is limited only by the camera acquisition rate. This implementation has allowed the imaging of the cortex of the brain of an awake behaving mouse at a speed as high as 10 Hz, but with limited penetration depth [50].** We have seen that different LSFM configurations have been developed in order to improve acquisition speed, resolution and penetration depth, but is a change in geometry really enough?

2.2. Overcoming the limitations of 'conventional' LSFM relying on Gaussian beams

A major trade-off between resolution and penetration depth is associated with the use of Gaussian beams in LSFM. In particular, an increase in resolution obtained by using a high NA objective results in a decrease in the Rayleigh range and thus axial resolution is compromised. The axial resolution which is dictated not only from the NA of the detection objective, but also from the thickness of the light sheet, is at least one order of magnitude bigger than the lateral resolution, which is dictated solely by the NA of the detection objective. In order to improve the optical sectioning ability it is necessary to circumvent the Rayleigh range. While using Gaussian beams, LSFM systems allow the imaging of fairly transparent specimens such as the larval zebrafish brain [34] where the ability to image in depth, turbid tissues is limited by the diffraction of light. The use of propagation invariant beams, such as Bessel and Airy beams in LSFM

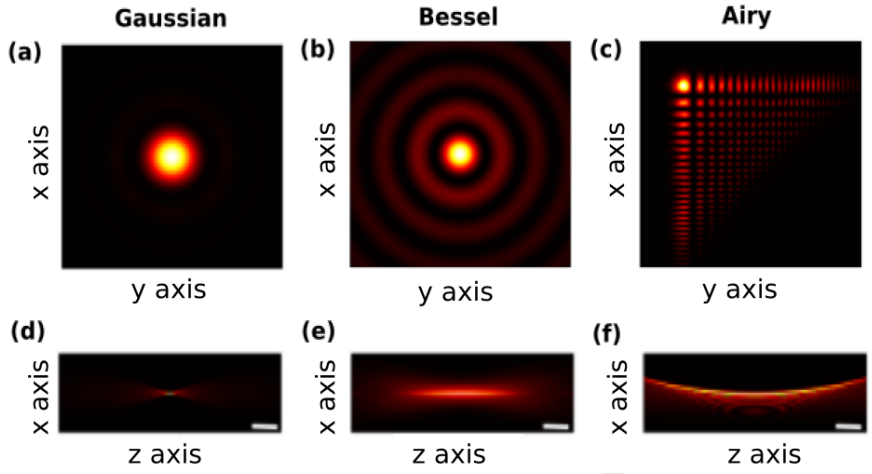

Figure 3: y-x cross-sectional profiles (z = 0) for a (a) Gaussian, a (b) Bessel ($\beta = 0.1$), and a (c) Airy ($\alpha = 2$) beam. z-x cross-sectional profiles (y = 0) for the same (d) Gaussian, (e) Bessel and (f) Airy beam propagating with parameters: $\lambda = 488$ nm, NA = 0.23, in air (n = 1). Scale bar: 50 μm.

overcomes these limitations providing a high resolution across a larger field of view [75, 76, 77] (see Figure 3).

An ideal Bessel beam is a propagation invariant light beam consisting of an infinite number of concentric rings covering an infinite distance and carrying an infinite amount of energy [78]. Despite the fact that such an ideal Bessel beam cannot be made, a "pseudo" Bessel beam having a finite number of rings and carrying a finite amount of energy but still possessing propagation invariant properties over an extended distance with respect to the Rayleigh range can be created experimentally. Bessel beams are obtained by passing a Gaussian beam, through a conical lens (axicon), by using the combination of an annular slit and lens, or by using diffractive optics techniques [79, 80, 81, 82, 83]. Even if the Fourier conjugate for a perfect ideal Bessel beam is an annulus, placing an annular aperture in the back focal plane of a lens to create a Bessel beam can lead to on-axis intensity rapid oscillatory behaviour [84]. The holographic generation of Bessel beams by using spatial light modulators (SLMs) is another

well established method and it also allows the generation of multiple beams simultaneously. However, the most efficient way of creating a Bessel beam is imposing a phase shift to an incident Gaussian beam by passing it through an axicon [85, 86]. By changing the angle of the axicon therefore, it is possible to control the Bessel beam core size.

The smaller core size, the self-healing properties and the propagation invariance of Bessel beams make them very good candidates for imaging thick non-transparent samples with high resolution[61]. However, if single photon illumination is used, the Bessel beam side lobes contribute to background noise and higher levels of phototoxicity [76]. In order to minimize these problems, it is possible to use 2P excitation in which the quadratic dependence of fluorescence from the illumination intensity allows the collection of signals only from the central core, or to block the detection of the side lobes on the camera sensor [76, 84, 87, 88, 89]. Another way of minimizing the effects of the Bessel light sheet side lobes is the use of structured illumination in which multiple Bessel beams interfere with each other creating a Bessel beam plane [90]. The use of structured illumination leads to the development of lattice light sheet microscopy (LLSM) in which, given the correct periodicity, diffraction interference between an array of Bessel beams allows the suppression of the Bessel rings producing an optical lattice [51]. This technique provides high axial resolution by delivering ultra-thin light sheets of $\sim 1\mu$m and high imaging speed at hundreds of planes per second while reducing photobleaching and phototoxicity by one to two orders of magnitude with respect to 1D scanned Bessel beams. However, its penetration depth is limited to $\sim$ 20-100 μm making it not suitable for imaging turbid and thick tissues, such as the mammalian brain [51]. This may be caused by a reduction of the k-space with respect to Bessel and Airy beams and therefore, of the LLSM 'self healing' properties. Lattices can in fact be generated by superimposing an opaque mask containing a set of slit apertures over the base ring pupil used for generating a Bessel beam, using just a few quasi-discrete wavevectors of the ring reducing considerably the former k-space [91].

An Airy beam, like a Bessel beam, also has a propagation invariant intensity

profile and exhibits 'self-healing', but tends to freely accelerate during propagation [92]. The beam profile possesses an inherent asymmetry. Airy beams can be obtained by passing a Gaussian beam through the Fourier transformation of a cubic phase [92, 93]. This can be done by using a spatial light modulator (SLM) or by using a custom made designed cubic phase mask [94, 95]. **The strength of the cubic phase modulation dictates the shape and properties of the Airy beam. Its propagation-invariant length increases with** $\mid \alpha \mid$ **being** α**=0 equivalent to a Gaussian beam.** However, it has recently been demonstrated that by simply controlling the tilting of a cylindrical lens, can induced aberrations such that they closely approximate the cubic modulation necessary to form an Airy light sheet [96].Vettenburg et al. [77] have shown that Airy beams yield thinner light sheets over larger FOVs when compared to Gaussian and Bessel beams of similar NA. They have also showed that in single photon LSFM, differently from the Bessel beam side lobes, the transverse Airy beam structure contributes positively to the imaging process. This is a great advantage over 1D Bessel techniques in which much of the florescence is rejected to improve image quality and therefore the light sheet intensity needs to be increased to achieve the same contrast. As the power of an Airy light sheet is spread out over a larger area with respect to an equivalent Gaussian light sheet, and because of the positive contribution of all its structures to imaging formation, the peak intensity is reduced and with it the photobleaching [77].

However, how much of the transverse Airy structure will be collected in-focus is dictated by the depth of field (DOF) of the detection lens, which increases with the decreasing of the detection lens NA. The detection lens DOF should be as large as possible to ensure that most of the Airy profile is within it. In this way all of the generated fluorescence contributes to the image and through the use of computational deconvolution resolution comparable to a Gaussian light sheet with equal NA can be obtained. High resolution images from raw data can be restored performing deconvolution by using a simple 1D Wiener filter applied along the axial direction of the images [77].

Due to the restriction imposed by the detection lens DOF most Airy LSFM has been performed with illumination and detection NA not higher than 0.4. For NA= 0.4 imaging with isotropic resolution of 800 nm across a FOV of 340 μm is achieved.

Airy LSFM seems to be very promising for imaging in turbid neural tissues. J. Nylk et al [97] carried out a comparison between Airy LSFM and Gaussian LSM showing three-fold improvement in image quality at a depth of 50 μm into mouse brain tissue most likely due to the 'self-healing' properties of the beam. They also tested the penetration depth in cleared samples with each beam type showing a 30% extended penetration depth when using an Airy light sheet. They recently developed the attenuation compensation of light field approach in which the intensity of the beam is changed upon its propagation enabling its strategical redistribution within the sample in order to maximize signal and minimize irradiation [98]. By using this method they were able to image an additional 70% dendritic spines in mouse brain tissue with respect to using a non compensated Airy beam.

3. Applications of light sheet fluorescence microscopy in neuroscience

The development of LSFM rendered possible the observation of phenomena that were not easily accessible before, such as the comprehensive quantitative analyses of cellular dynamics in entire developing organisms. In particular, the development of four-lenses LSFM setups, which records multiple views of the specimen simultaneously, allowed recording cellular dynamics in complex biological systems, such as Drosophila melanogaster embryos, and in-vivo imaging of the developing nervous system [66]. The combination of LSFM with advanced computational tools also allowed automated cellular phenotyping and mapping of gene expression dynamics for entire embryos [66]. One of the main challenges in developmental and regenerative biology is the study of lineages of cells, which determine their avail-

able differentiation fates. LSFM allowed recording nuclei localization and tracking of majority of cell movements in entire wild-type and mutant zebrafish embryos in the first 24 hours of development [60]. The lineage of cells giving rise to a specific organ was also observed, at a later stage of development, during organogenesis of the posterior lateral line in zebrafish [99]. Its capability of fast and low phototoxic imaging makes LSFM also a suitable tool for observing the formation of the zebrafish retinal ganglion cell layer, the first step of neuronal lamination in the retina [100]. LSFM has recently found its application also in better understanding the dynamic of axon-glia cells interaction during neuronal regeneration consequent to injury in the nervous system. In particular, the combination of lattice light sheet microscopy with laser microsurgery, genetic analysis and high-resolution intravital imaging was used to study the interaction between Schwann cells and sensory neurons in a zebrafish model of neurotrauma [101]. This technique demonstrated also to be an excellent tool for a better understanding of cell behaviour and disease in complex 3D neuronal cultures resembling physiological conditions, such as organoids and neurospheres [102]. Even though the application of LSFM in developmental biology and axonal morphogenesis, in understanding axon-glia cells interaction and in imaging 3D neuronal cultures is increasing, these research fields are not mainstream at this time. The two main fields of research in which LSFM has found its application are the acquisition of functional imaging of the nervous system and the acquisition of the morphology of cleared brains and will be discussed in the next two sections.

3.1. Functional Imaging of the nervous system

Coupling LSFM with the new generation of genetically encoded calcium indicators has facilitated high speed and high resolution imaging of large neural populations leading to new insights into CNS [34]. Even though the first

functional imaging experiments using SPIM were performed on excised mice's vomeronasal organs with a penetration depth limited to ~ 150 μm, they shown the incredible potential of LSFM recording an unprecedented number of neurons simultaneously [35]. Panier et al [33] used SPIM to collect functional images of large fractions of the brain volume of 5-9 day old zebrafish larvae at 20 Hz with near single cell resolution. Ahrens et al. [34] recorded the activity of the entire brain of the larval zebrafish *in-vivo* by using the genetically encoded calcium indicator GCaMP5G. They were capable of capturing the activity of more than 80% of all neurons at single cell resolution by covering a volume of 800 x 600 x 200 um^3 in 1.3 s (see Figure 4). However, both SPIM and **four-lens** LSFM implementations could not be combined with visually driven behaviour, due to the fact that the light sheet scans over the zebrafish eye confounding eye stimulation. To overcome this limitation, multiple excitation beams acquired from different brain regions and avoiding direct exposure of the zebrafish retina or two-photon excitation could be used [103, 104].

Spatially isotropic whole brain functional imaging in larval zebrafish at 1 Hz was also collected by using IsoView LSFM [67]. The decay time of GECIs is on the order of 1 to 2 s, however, their activation time is about 100 ms, therefore, acquisition speed as high as 100 Hz or even better is necessary to record fast synaptic events. Imaging of axons and dendrites in a living mammalian brain slice, over an area of 300 x 300 μm at 100 Hz was collected by Yang et al [70]. However, their image of rapid post-synaptic events was acquired in the single plane mode because 3D imaging requires the movement of the sample by a piezoelectric stage, and this requirement reduces significantly the acquisition speed. Different LSFM approaches to enable fast volumetric imaging of activity in neuronal populations have been developed over time. One approach used is coupling the position of the illumination sheet with the one of the collection objective avoiding sample movement [35, 44, 105]. **However, this approach leads to acquisition speed limited to 10 volume/sec in SPIM setups due to the mechanical motion of the piezo-coupled microscope objective limiting the scanning frequency.** Extension of the depth of field

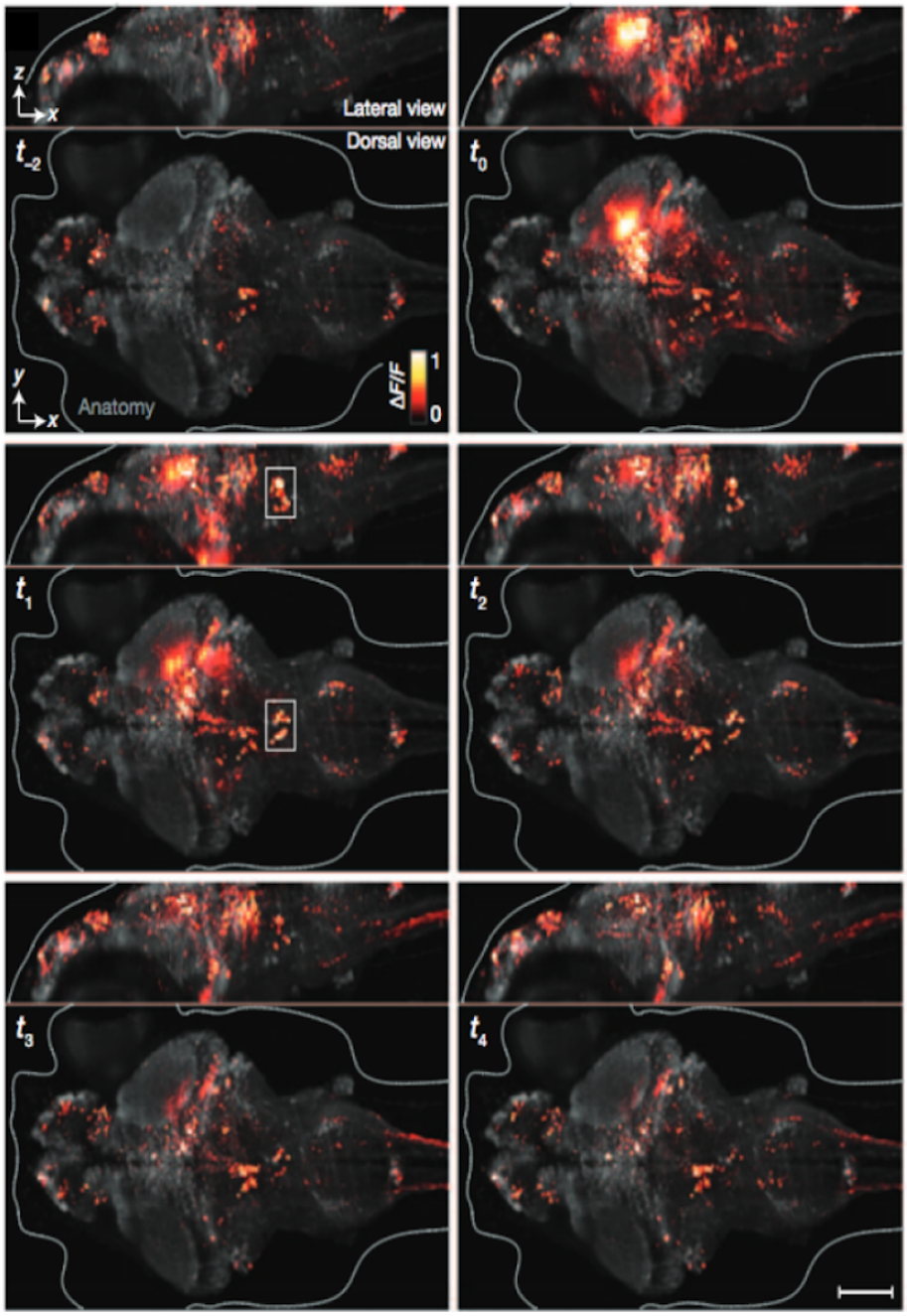

Figure 4: Functional imaging of neuronal activity of the entire brain of the larval zebrafish with cellular resolution. Panels represent whole-brain volumes recorded in intervals of 1.39 s. The dorsal and lateral projections of whole-brain, neuron-level functional activity, is reported by the genetically encoded calcium indicator GCaMP5G via changes in fluorescence intensity. Image adapted with permission from [34]

of the detection objective by introducing a spherical aberration that results in PSF elongation imaging or by adding an optical element that provides for cubic phase pupil encoding has been used as alternative approach [48, 49]. Multi-plane calcium imaging in the larval zebrafish brain at 33 Hz has been demonstrated by extending the depth of field using a static cubic phase mask[49]. However, optical efficiency and the signal to noise ratio are compromised because of the elongated point spread function along the detection axis. **Single 3D imaging of the dendritic arbor of a living pyramidal neuron, scanned at a depth of 20 μm, at 50 Hz has been recently acquired by Haslehurst et al. [106] by modifying the setup described in [70]. They achieved this capability by synchronizing the 1D galvo mirror in the illumination path with the ETL in the detection path, while setting the camera's exposure time equal to the period in which the light sheet and the detection objectives focal plane both make one complete scan through the detection axis. They made the assumption that the positions of neurons and their synapses is known and remain unchanged during each imaging session and so there is no necessity of constantly monitoring and tracking their 3D positions. In this way the 3D structure of a neuron can be obtained by acquiring an image stack only once.**

3.2. Imaging of entire cleared mammalian brains

One of the main challenges in neuroscience is imaging an entire brain with sub-cellular resolution. The high absorption and strong scattering of light in biological tissues makes it difficult to acquire fluorescent images of large volumes with a high spatial resolution. As already mentioned in 1.1, optical clearing circumvents this problem rendering tissues transparent and thus enhancing imaging. LSFM, which samples entire planes in the specimen with each camera frame acquisition, combined with tissue clearing, enables imaging of volumes of large specimens with micrometer resolution within minutes.

Dodt et al [46] performed the first demonstration of LSFM on cleared mouse brains. They developed a method called BABB with which they cleared the

specimen by dipping it in a medium with the same refractive index as protein. In this way, the refractive indices of intra- and extracellular compartments become the same, allowing the light to pass through the sample without scattering. They imaged the sample from top and bottom, after a 180 rotation, directly in the clearing solution with two illumination arms and one detection objective. They were capable of imaging GFP expressing neurons in whole brains of transgenic mice and obtaining anatomical details of the whole brain visualizing the shape of the hippocampus. They could even discern GFP-labelled neuronal soma and dendrites within the hippocampus through the overlying neocortex. However, for objects bigger than 2 mm they could not reach sub-micrometer resolution and had limited penetration depth due to the specimens autofluorescence. Furthermore, they could not image whole brains of mice older than 2 weeks as heavily myelinated structures do not become transparent rendering the scattering of light a limitation for resolution and penetration depth. **The BABB method was then improved to 3DISCO developed by Ertürk et al. [107] and the clearing method using a mixture of tetrahydrofuran and dibenzyl ether developed by Becker et al. [108], which yielded improved stability of GFP.** Other clearing methods based on the removal of lipids, which are the main source of scattering in tissues, and/or adjustment of the refractive index difference between lipids and the surrounding areas were later developed [47, 109, 110, 111, 112]. Among these methods CLARITY achieves lipid extraction in fixed samples through electrophoresis and replaces them with nanoporous hydrogel increasing tissue permeability while preserving its structure and enabling diffusion of molecular probes deep into intact tissue [111]. The application of this clearing method in LSFM was demonstrated by Tomer et al. [113] who imaged CLARITY cleared mouse brains achieving subcellular resolution (see Figure 5 (d) to (l)). With CLARITY based protocols, refractive index mismatches remain and optical distortions have been reported [111].

Later, Susaki et al [47] developed a less aggressive clearing technique called CUBIC. This approach requires only immersion of the tissue in two reagents

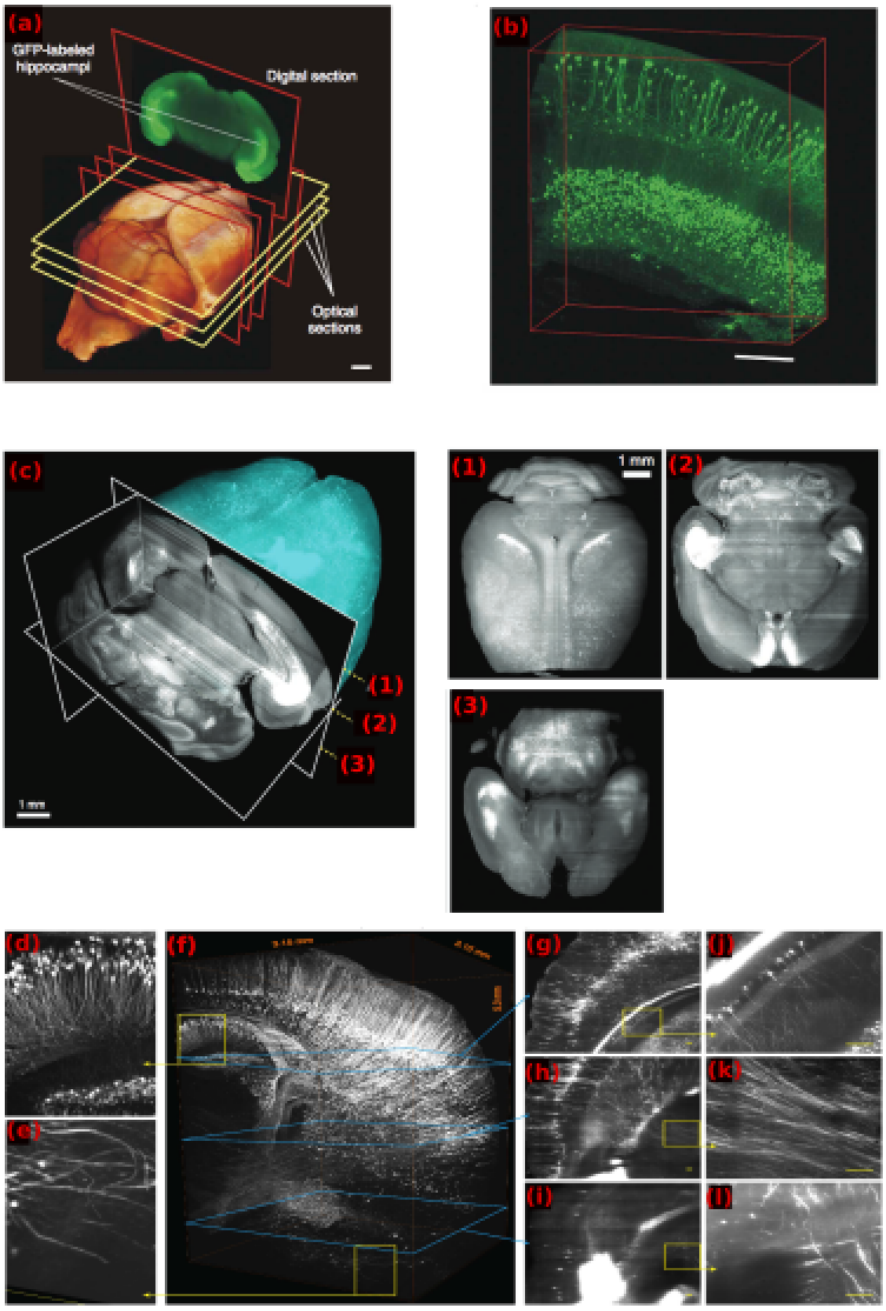

Figure 5: Imaging of cleared mouse brains. (a) Surface of a whole mouse brain reconstructed from 550 optical sections and taken by using Ultramicroscopy. Scale bar = 1 mm. (b) 3D reconstruction of part of a whole hippocampus of the brain imaged in (a). Scale bar = 200 μm. (c) 3D reconstruction of an entire mouse brain cleared with 3DISCO from GFP-M line mice using ultramicroscopy; (1-3) The horizontal projections ($\sim$ 100 μm) from the cleared brain at different depths marked in (c).(f) High-resolution imaging of a Thy1-eYFP mouse brain cleared by using CLARITY;(d-e) Magnified views of the regions in (f) highlighted by yellow boxes;(g-i) Magnified views of the regions in (f) highlighted by blue planes;(j-l) Magnified views of the regions, highlighted by yellow boxes, in (g),(h) and (i), respectively. (a) and (b) were adapted with permission from [46]. (c) was adapted with permission from [107].(d) through (l) were adapted with permission from [113].

and it is well suited for use with different types of fluorescence proteins including GFP. Using this technique, they performed imaging of cleared mice brains and were also capable of imaging a 3 day old marmoset brain, with well preserved cell structures such as axons and spines. However, some opacity remained visible in CUBIC cleared brains. A slightly better transparency seems to be obtained by using the solvent-based dehydration FluoClearBABB protocol to clear mice brains [114]. CLARITY, CUBIC and FluoClearBABB approaches have been tested and compared for LSFM imaging of cleared adult transgenic Thy1-GFP rat brain, with the FluoClearBABB method resulting in being superior to the other techniques [115]. While for 3 mm brain slices both CLARITY and FluoClearBABB methods yield good transparency, deep brain structures were revealed only using the FluoClearBABB approach. Furthermore, while tissues treated with the CLARITY and CUBIC methods increase in size, the ones cleared with the FluoClearBABB protocol undergo volumetric reduction. A reduction in tissue size up to 65% and therefore an increased LSFM imaging acquisition speed is reported to be obtained by using an organic solvent based clearing method called ultimate DISCO. LSFM images of neuronal connections and vasculature within the entire body of adult mice have been acquired by using this clearing method [116]. Even though LSFM images of intact adult mouse brain have been acquired with dendritic spine resolution, tissue shrinkage leads to 30% decreased resolution in one dimension. Recently, other clearing protocols for the visualization of whole mouse brain vasculature system have been developed [117, 118].

Although the development of optical clearing methods render possible the observation of entire fixed brains there is a compelling necessity for in-vivo brain imaging. As previously mentioned, this cannot be easily obtained with LSFM techniques using two orthogonal objectives which dictate a limitation in the sample geometry. Instead, the development of single objective LSFM techniques, such as SCAPE, is a potential route for imaging neuronal activity in live mouse brain through a cranial window [50].

4. Outlook

The application of light sheet fluorescence microscopy in neuroscience has led to major advances in the past few years. Major breakthroughs have occurred thanks to the possibility of imaging *in-vivo* the development of the CNS and in acquiring functional and morphological images of whole mammalian brains with sub cellular resolution. Future directions in the application of LSFM in neuroscience will see the further development of single objective implementations in order to overcome the limitations on sample accessibility and acquisition speed, imposed by multiview LSFM. This kind of geometry would also be particularly suited for use with microfluidics chips in order to monitor single cell growth or for developmental imaging of the CNS of multiple embryos. Of interest would also be coupling flow based technology for *in-vivo* monitoring of drug effects on the CNS.

The possibility of selectively labelling different neurons makes feasible coupling LSFM with optogenetics. In optogenetics, photosynthetic proteins expressed in neurons convert light into electricity signal. Light is then used to either turn on or off these neurons activity. The goal is to control electric activity in specific neurons and not others within a network, in order to figure out, for example, how a network of neurons contribute to behavior. It is also be possible to establish potentially which cells contribute to a disease state or which are switched off in a disease state.

The use of existing propagation invariant beams has made possible increasing the penetration depth in non-transparent samples, and the development of new more efficient beams could render imaging in even deeper tissues. However, in depth *in-vivo* imaging would require the further development of fibre based LSFM [119]. Engelbrecht et al. [120] demonstrated the potential of a miniaturized fibre optics light sheet imaging GABAergic interneurons from transgenic GAD67-GFP mice in paraformaldehyde-fixed brain tissue and *in-vivo*. They delivered the excitation light through a single-mode optical fiber and collected the fluorescence emission orthogonally to the illumination through a gradient-

index lens assembly and a coherent fiber bundle. They created the light sheet by using a 1 mm cylindrical gradient-index lens and a right-angle microprism. This method allowed cell discrimination at 125 μm depth into the mouse brain. Of particular interest is to couple the previously mentioned attenuation compensation of light field approach [98] with self-learning algorithms to develop a new generation of smart LSFM in which not only acquisition parameters are optimized (e.g. Autopilot [121]), but also the penetration depth thorough light exposure control.

Another aspect to be considered is the acquisition of very large data sets (on the order of terabytes) which poses unprecedented challenges regarding data management, analysis, and mining [122]. Therefore, improvement in data storage and image processing will be required. This could be achieved with smart acquisition of only meaningful data and background rejection. Improvement of algorithms for fast reconstruction of cell positions, nuclei/cell boundaries and cell tracking in developmental images will also be necessary. The complexity of functional images will require further development of automated computational approaches, such as machine learning and deep machine learning, to extract biological information. Despite the further developments and improvements to be made, the application of LSFM in neuroscience has already shown its huge potential, and many routes for future applications in this field can already be envisaged.

Acknowledgements

We thank the UK Engineering and Physical Sciences Research Council for funding through grants EP/R004854/1 and EP/P030017/1.

References

[1] D. Gunn-Moore, O. Kaidanovich-Beilin, M. C. G. Iradi, F. Gunn-Moore, S. Lovestone, Alzheimers disease in humans and other animals: A con-

sequence of postreproductive life span and longevity rather than aging, Alzheimers & Dementia 1 (2017) 10.

[2] A. P. Alivisatos, M. Chun, G. M. Church, R. J. Greenspan, M. L. Roukes, R. Yuste, The brain activity map project and the challenge of functional connectomics, Neuron 74 (2012) 970–974.

[3] Y. G. Maguire, M. G. Shapiro, T. R. Cybulski, J. I. Glaser, D. Amodei, P. B. Stranges, R. Kalhor, D. A. Dalrymple, D. Seo, E. Alon, et al., Physical principles for scalable neural recording, Frontiers in Computational Neuroscience 7 (2013) 137.

[4] A. Grinvald, R. Hildesheim, Vsdi: a new era in functional imaging of cortical dynamics, Nature Reviews Neuroscience 5 (2004) 874.

[5] A. Holtmaat, K. Svoboda, Experience-dependent structural synaptic plasticity in the mammalian brain, Nature Reviews Neuroscience 10 (2009) 647.

[6] J. W. Wang, A. M. Wong, J. Flores, L. B. Vosshall, R. Axel, Two-photon calcium imaging reveals an odor-evoked map of activity in the fly brain, Cell 112 (2003) 271–282.

[7] J. Grutzendler, N. Kasthuri, W.-B. Gan, Long-term dendritic spine stability in the adult cortex, Nature 420 (2002) 812.

[8] T. Schrödel, R. Prevedel, K. Aumayr, M. Zimmer, A. Vaziri, Brain-wide 3d imaging of neuronal activity in caenorhabditis elegans with sculpted light, Nature Methods 10 (2013) 1013.

[9] M. B. Ahrens, J. M. Li, M. B. Orger, D. N. Robson, A. F. Schier, F. Engert, R. Portugues, Brain-wide neuronal dynamics during motor adaptation in zebrafish, Nature 485 (2012) 471.

[10] R. Portugues, C. E. Feierstein, F. Engert, M. B. Orger, Whole-brain activity maps reveal stereotyped, distributed networks for visuomotor behavior, Neuron 81 (2014) 1328–1343.

[11] F. Helmchen, W. Denk, Deep tissue two-photon microscopy, Nature Methods 2 (2005) 932.

[12] J. Huisken, J. Swoger, F. Del Bene, J. Wittbrodt, E. H. Stelzer, Optical sectioning deep inside live embryos by selective plane illumination microscopy, Science 305 (2004) 1007–1009.

[13] S. Quirin, J. Jackson, D. S. Peterka, R. Yuste, Simultaneous imaging of neural activity in three dimensions, Frontiers in Neural Circuits 8 (2014) 29.

[14] F. Anselmi, C. Ventalon, A. Bègue, D. Ogden, V. Emiliani, Three-dimensional imaging and photostimulation by remote-focusing and holographic light patterning, Proceedings of the National Academy of Sciences 108 (2011) 19504–19509.

[15] V. Nikolenko, B. O. Watson, R. Araya, A. Woodruff, D. S. Peterka, R. Yuste, Slm microscopy: scanless two-photon imaging and photostimulation using spatial light modulators, Frontiers in Neural Circuits 2 (2008) 5.

[16] I.-W. Chen, E. Ronzitti, B. R. Lee, T. L. Daigle, H. Zeng, E. Papagiakoumou, V. Emiliani, Parallel holographic illumination enables sub-millisecond two-photon optogenetic activation in mouse visual cortex in vivo, bioRxiv (2018) 250795.

[17] M. Žurauskas, O. Barnstedt, M. Frade-Rodriguez, S. Waddell, M. J. Booth, Rapid adaptive remote focusing microscope for sensing of volumetric neural activity, Biomedical Optics Express 8 (2017) 4369–4379.

[18] A. R. Mardinly, N. C. Pegard, I. Oldenburg, S. Sridharan, R. Hakim, L. Waller, H. Adesnik, 3d all-optical control of functionally defined neurons with cellular resolution and sub-millisecond precision, in: Optics and the Brain, Optical Society of America, 2017, pp. BrM3B–4.

[19] G. D. Reddy, K. Kelleher, R. Fink, P. Saggau, Three-dimensional random access multiphoton microscopy for functional imaging of neuronal activity, Nature Neuroscience 11 (2008) 713.

[20] R. Salome, Y. Kremer, S. Dieudonne, J.-F. Léger, O. Krichevsky, C. Wyart, D. Chatenay, L. Bourdieu, Ultrafast random-access scanning in two-photon microscopy using acousto-optic deflectors, Journal of Neuroscience Methods 154 (2006) 161–174.

[21] G. Katona, G. Szalay, P. Maák, A. Kaszás, M. Veress, D. Hillier, B. Chiovini, E. S. Vizi, B. Roska, B. Rózsa, Fast two-photon in vivo imaging with three-dimensional random-access scanning in large tissue volumes, Nature Methods 9 (2012) 201.

[22] B. F. Grewe, D. Langer, H. Kasper, B. M. Kampa, F. Helmchen, High-speed in vivo calcium imaging reveals neuronal network activity with near-millisecond precision, Nature Methods 7 (2010) 399.

[23] R. J. Cotton, E. Froudarakis, P. Storer, P. Saggau, A. S. Tolias, Three-dimensional mapping of microcircuit correlation structure, Frontiers in Neural Circuits 7 (2013) 151.

[24] J. Tønnesen, G. Katona, B. Rózsa, U. V. Nägerl, Spine neck plasticity regulates compartmentalization of synapses, Nature Neuroscience 17 (2014) 678.

[25] I. Izeddin, C. G. Specht, M. Lelek, X. Darzacq, A. Triller, C. Zimmer, M. Dahan, Super-resolution dynamic imaging of dendritic spines using a low-affinity photoconvertible actin probe, PloS one 6 (2011) e15611.

[26] S. A. Jones, S.-H. Shim, J. He, X. Zhuang, Fast, three-dimensional super-resolution imaging of live cells, Nature Methods 8 (2011) 499.

[27] G. Giannone, E. Hosy, F. Levet, A. Constals, K. Schulze, A. I. Sobolevsky, M. P. Rosconi, E. Gouaux, R. Tampé, D. Choquet, et al., Dynamic

superresolution imaging of endogenous proteins on living cells at ultra-high density, Biophysical Journal 99 (2010) 1303–1310.

[28] C. Tardin, L. Cognet, C. Bats, B. Lounis, D. Choquet, Direct imaging of lateral movements of ampa receptors inside synapses, The EMBO Journal 22 (2003) 4656–4665.

[29] D. Nair, E. Hosy, J. D. Petersen, A. Constals, G. Giannone, D. Choquet, J.-B. Sibarita, Super-resolution imaging reveals that ampa receptors inside synapses are dynamically organized in nanodomains regulated by psd95, Journal of Neuroscience 33 (2013) 13204–13224.

[30] M. Levoy, R. Ng, A. Adams, M. Footer, M. Horowitz, Light field microscopy, in: ACM Transactions on Graphics (TOG), volume 25, ACM, 2006, pp. 924–934.

[31] M. Broxton, L. Grosenick, S. Yang, N. Cohen, A. Andalman, K. Deisseroth, M. Levoy, Wave optics theory and 3-d deconvolution for the light field microscope, Optics Express 21 (2013) 25418–25439.

[32] R. Prevedel, Y.-G. Yoon, M. Hoffmann, N. Pak, G. Wetzstein, S. Kato, T. Schrödel, R. Raskar, M. Zimmer, E. S. Boyden, et al., Simultaneous whole-animal 3d imaging of neuronal activity using light-field microscopy, Nature Methods 11 (2014) 727.

[33] T. Panier, S. Romano, R. Olive, T. Pietri, G. Sumbre, R. Candelier, G. Debrégeas, Fast functional imaging of multiple brain regions in intact zebrafish larvae using selective plane illumination microscopy, Frontiers in Neural Circuits 7 (2013) 65.

[34] M. B. Ahrens, M. B. Orger, D. N. Robson, J. M. Li, P. J. Keller, Whole-brain functional imaging at cellular resolution using light-sheet microscopy, Nature Methods 10 (2013) 413.

[35] T. F. Holekamp, D. Turaga, T. E. Holy, Fast three-dimensional fluorescence imaging of activity in neural populations by objective-coupled planar illumination microscopy, Neuron 57 (2008) 661–672.

[36] P. P. Laissue, R. A. Alghamdi, P. Tomancak, E. G. Reynaud, H. Shroff, Assessing phototoxicity in live fluorescence imaging, Nature Methods 14 (2017) 657.

[37] F. Pampaloni, N. Ansari, P. Girard, E. H. Stelzer, Light sheet-based fluorescence microscopy (lsfm) reduces phototoxic effects and provides new means for the modern life sciences, in: European Conference on Biomedical Optics, Optical Society of America, 2011, p. 80860Y.

[38] M. Jemielita, M. J. Taormina, A. DeLaurier, C. B. Kimmel, R. Parthasarathy, Comparing phototoxicity during the development of a zebrafish craniofacial bone using confocal and light sheet fluorescence microscopy techniques, Journal of Biophotonics 6 (2013) 920–928.

[39] J. Icha, M. Weber, J. C. Waters, C. Norden, Phototoxicity in live fluorescence microscopy, and how to avoid it, Bioessays 39 (2017).

[40] E. G. Reynaud, U. Kržič, K. Greger, E. H. Stelzer, Light sheet-based fluorescence microscopy: more dimensions, more photons, and less photodamage, HFSP Journal 2 (2008) 266–275.

[41] E. H. Stelzer, Light-sheet fluorescence microscopy for quantitative biology, Nature Methods 12 (2015) 23–26.

[42] R. M. Power, J. Huisken, A guide to light-sheet fluorescence microscopy for multiscale imaging, Nature Methods 14 (2017) 360.

[43] L. Leung, A. V. Klopper, S. W. Grill, W. A. Harris, C. Norden, Apical migration of nuclei during g2 is a prerequisite for all nuclear motion in zebrafish neuroepithelia, Development 138 (2011) 5003–5013.

[44] Y. Wu, A. Ghitani, R. Christensen, A. Santella, Z. Du, G. Rondeau, Z. Bao, D. Colón-Ramos, H. Shroff, Inverted selective plane illumination microscopy (ispim) enables coupled cell identity lineaging and neurodevelopmental imaging in caenorhabditis elegans, Proceedings of the National Academy of Sciences 108 (2011) 17708–17713.

[45] Y. Wu, R. Christensen, D. Colón-Ramos, H. Shroff, Advanced optical imaging techniques for neurodevelopment, Current Opinion in Neurobiology 23 (2013) 1090–1097.

[46] H.-U. Dodt, U. Leischner, A. Schierloh, N. Jährling, C. P. Mauch, K. Deininger, J. M. Deussing, M. Eder, W. Zieglgänsberger, K. Becker, Ultramicroscopy: three-dimensional visualization of neuronal networks in the whole mouse brain, Nature Methods 4 (2007) 331.

[47] E. A. Susaki, K. Tainaka, D. Perrin, F. Kishino, T. Tawara, T. M. Watanabe, C. Yokoyama, H. Onoe, M. Eguchi, S. Yamaguchi, et al., Whole-brain imaging with single-cell resolution using chemical cocktails and computational analysis, Cell 157 (2014) 726–739.

[48] R. Tomer, M. Lovett-Barron, I. Kauvar, A. Andalman, V. M. Burns, S. Sankaran, L. Grosenick, M. Broxton, S. Yang, K. Deisseroth, Sped light sheet microscopy: fast mapping of biological system structure and function, Cell 163 (2015) 1796–1806.

[49] S. Quirin, N. Vladimirov, C.-T. Yang, D. S. Peterka, R. Yuste, M. B. Ahrens, Calcium imaging of neural circuits with extended depth-of-field light-sheet microscopy, Optics Letters 41 (2016) 855–858.

[50] M. B. Bouchard, V. Voleti, C. S. Mendes, C. Lacefield, W. B. Grueber, R. S. Mann, R. M. Bruno, E. M. Hillman, Swept confocally-aligned planar excitation (scape) microscopy for high-speed volumetric imaging of behaving organisms, Nature Photonics 9 (2015) 113.

[51] B.-C. Chen, W. R. Legant, K. Wang, L. Shao, D. E. Milkie, M. W. Davidson, C. Janetopoulos, X. S. Wu, J. A. Hammer, Z. Liu, et al., Lattice light-sheet microscopy: imaging molecules to embryos at high spatiotemporal resolution, Science 346 (2014) 1257998.

[52] V. V. Tuchin, I. L. Maksimova, D. A. Zimnyakov, I. L. Kon, A. H. Mavlyutov, A. A. Mishin, Light propagation in tissues with controlled optical properties, Journal of Biomedical Optics 2 (1997) 401–418.

[53] V. Tuchin, G. Altshuler, A. Gavrilova, A. Pravdin, D. Tabatadze, J. Childs, I. Yaroslavsky, Optical clearing of skin using flashlamp-induced enhancement of epidermal permeability, Lasers in Surgery and Medicine 38 (2006) 824–836.

[54] D. Zhu, K. V. Larin, Q. Luo, V. V. Tuchin, Recent progress in tissue optical clearing, Laser & Photonics Reviews 7 (2013) 732–757.

[55] H. Siedentopf, R. Zsigmondy, Uber sichtbarmachung und größenbestimmung ultramikoskopischer teilchen, mit besonderer anwendung auf goldrubingläser, Annalen der Physik 315 (1902) 1–39.

[56] J. Swoger, P. Verveer, K. Greger, J. Huisken, E. H. Stelzer, Multi-view image fusion improves resolution in three-dimensional microscopy, Optics Express 15 (2007) 8029–8042.

[57] A. Kaufmann, M. Mickoleit, M. Weber, J. Huisken, Multilayer mounting enables long-term imaging of zebrafish development in a light sheet microscope, Development 139 (2012) 3242–3247.

[58] E. J. Gualda, H. Pereira, T. Vale, M. F. Estrada, C. Brito, N. Moreno, Spim-fluid: open source light-sheet based platform for high-throughput imaging, Biomedical optics Express 6 (2015) 4447–4456.

[59] P. Strnad, S. Gunther, J. Reichmann, U. Krzic, B. Balazs, G. De Medeiros, N. Norlin, T. Hiiragi, L. Hufnagel, J. Ellenberg, Inverted light-sheet micro-

scope for imaging mouse pre-implantation development, Nature Methods 13 (2016) 139.

[60] P. J. Keller, A. D. Schmidt, J. Wittbrodt, E. H. Stelzer, Reconstruction of zebrafish early embryonic development by scanned light sheet microscopy, Science 322 (2008) 1065–1069.

[61] F. O. Fahrbach, A. Rohrbach, Propagation stability of self-reconstructing bessel beams enables contrast-enhanced imaging in thick media, Nature Communications 3 (2012) 632.

[62] T. V. Truong, W. Supatto, D. S. Koos, J. M. Choi, S. E. Fraser, Deep and fast live imaging with two-photon scanned light-sheet microscopy, Nature Methods 8 (2011) 757.

[63] A. Rohrbach, Artifacts resulting from imaging in scattering media: a theoretical prediction, Optics Letters 34 (2009) 3041–3043.

[64] J. Huisken, D. Y. Stainier, Even fluorescence excitation by multidirectional selective plane illumination microscopy (mspim), Optics Letters 32 (2007) 2608–2610.

[65] U. Krzic, S. Gunther, T. E. Saunders, S. J. Streichan, L. Hufnagel, Multiview light-sheet microscope for rapid in toto imaging, Nature Methods 9 (2012) 730.

[66] R. Tomer, K. Khairy, F. Amat, P. J. Keller, Quantitative high-speed imaging of entire developing embryos with simultaneous multiview light-sheet microscopy, Nature Methods 9 (2012) 755.

[67] R. K. Chhetri, F. Amat, Y. Wan, B. Höckendorf, W. C. Lemon, P. J. Keller, Whole-animal functional and developmental imaging with isotropic spatial resolution, Nature Methods 12 (2015) 1171.

[68] B. Schmid, G. Shah, N. Scherf, M. Weber, K. Thierbach, C. P. Campos, I. Roeder, P. Aanstad, J. Huisken, High-speed panoramic light-sheet

microscopy reveals global endodermal cell dynamics, Nature Communications 4 (2013) 2207.

[69] P. G. Pitrone, J. Schindelin, L. Stuyvenberg, S. Preibisch, M. Weber, K. W. Eliceiri, J. Huisken, P. Tomancak, Openspim: an open-access light-sheet microscopy platform, Nature Methods 10 (2013) 598.

[70] Z. Yang, P. Haslehurst, S. Scott, N. Emptage, K. Dholakia, A compact light-sheet microscope for the study of the mammalian central nervous system, Scientific Reports 6 (2016) 26317.

[71] Y. Wu, P. Wawrzusin, J. Senseney, R. S. Fischer, R. Christensen, A. Santella, A. G. York, P. W. Winter, C. M. Waterman, Z. Bao, et al., Spatially isotropic four-dimensional imaging with dual-view plane illumination microscopy, Nature Biotechnology 31 (2013) 1032.

[72] F. O. Fahrbach, F. F. Voigt, B. Schmid, F. Helmchen, J. Huisken, Rapid 3d light-sheet microscopy with a tunable lens, Optics Express 21 (2013) 21010–21026.

[73] O. E. Olarte, J. Andilla, D. Artigas, P. Loza-Alvarez, Decoupled illumination detection in light sheet microscopy for fast volumetric imaging, Optica 2 (2015) 702–705.

[74] C. Dunsby, Optically sectioned imaging by oblique plane microscopy, Optics Express 16 (2008) 20306–20316.

[75] F. O. Fahrbach, P. Simon, A. Rohrbach, Microscopy with self-reconstructing beams, Nature Photonics 4 (2010) 780.

[76] T. A. Planchon, L. Gao, D. E. Milkie, M. W. Davidson, J. A. Galbraith, C. G. Galbraith, E. Betzig, Rapid three-dimensional isotropic imaging of living cells using bessel beam plane illumination, Nature Methods 8 (2011) 417.

[77] T. Vettenburg, H. I. Dalgarno, J. Nylk, C. Coll-Lladó, D. E. Ferrier, T. Čižmár, F. J. Gunn-Moore, K. Dholakia, Light-sheet microscopy using an airy beam, Nature Methods 11 (2014) 541.

[78] J. Durnin, Exact solutions for nondiffracting beams. i. the scalar theory, JOSA A 4 (1987) 651–654.

[79] J. Durnin, J. Miceli Jr, J. Eberly, Diffraction-free beams, Physical Review Letters 58 (1987) 1499.

[80] A. Vasara, J. Turunen, A. T. Friberg, Realization of general nondiffracting beams with computer-generated holograms, JOSA A 6 (1989) 1748–1754.

[81] N. Chattrapiban, E. A. Rogers, D. Cofield, W. T. Hill III, R. Roy, Generation of nondiffracting bessel beams by use of a spatial light modulator, Optics Letters 28 (2003) 2183–2185.

[82] J. Leach, G. M. Gibson, M. J. Padgett, E. Esposito, G. McConnell, A. J. Wright, J. M. Girkin, Generation of achromatic bessel beams using a compensated spatial light modulator, Optics Express 14 (2006) 5581–5587.

[83] D. McGloin, K. Dholakia, Bessel beams: diffraction in a new light, Contemporary Physics 46 (2005) 15–28.

[84] M. Mazilu, D. J. Stevenson, F. Gunn-Moore, K. Dholakia, Light beats the spread:non-diffracting beams, Laser & Photonics Reviews 4 (2010) 529–547.

[85] G. Indebetouw, Nondiffracting optical fields: some remarks on their analysis and synthesis, JOSA A 6 (1989) 150–152.

[86] J. H. McLeod, The axicon: a new type of optical element, JOSA 44 (1954) 592–597.

[87] C. T. Brown, D. J. Stevenson, X. Tsampoula, C. McDougall, A. A. Lagatsky, W. Sibbett, F. J. Gunn-Moore, K. Dholakia, Enhanced operation

of femtosecond lasers and applications in cell transfection, Journal of Biophotonics 1 (2008) 183–199.

[88] F. O. Fahrbach, V. Gurchenkov, K. Alessandri, P. Nassoy, A. Rohrbach, Light-sheet microscopy in thick media using scanned bessel beams and two-photon fluorescence excitation, Optics Express 21 (2013) 13824–13839.

[89] P. Zhang, M. E. Phipps, P. M. Goodwin, J. H. Werner, Light-sheet microscopy by confocal line scanning of dual-bessel beams, Journal of Biomedical Optics 21 (2016) 100502.

[90] L. Gao, L. Shao, B.-C. Chen, E. Betzig, 3d live fluorescence imaging of cellular dynamics using bessel beam plane illumination microscopy, Nature Protocols 9 (2014) 1083.

[91] O. E. Olarte, J. Andilla, E. J. Gualda, P. Loza-Alvarez, Light-sheet microscopy: a tutorial, Adv. Opt. Photon. 10 (2018) 111–179.

[92] G. Siviloglou, J. Broky, A. Dogariu, D. Christodoulides, Observation of accelerating airy beams, Physical Review Letters 99 (2007) 213901.

[93] J. Baumgartl, M. Mazilu, K. Dholakia, Optically mediated particle clearing using airy wavepackets, Nature Photonics 2 (2008) 675.

[94] P. Polynkin, M. Kolesik, J. V. Moloney, G. A. Siviloglou, D. N. Christodoulides, Curved plasma channel generation using ultraintense airy beams, Science 324 (2009) 229–232.

[95] P. Polynkin, M. Kolesik, J. Moloney, Filamentation of femtosecond laser airy beams in water, Physical Review Letters 103 (2009) 123902.

[96] D. Papazoglou, S. Suntsov, D. Abdollahpour, S. Tzortzakis, Tunable intense airy beams and tailored femtosecond laser filaments, Physical Review A 81 (2010) 061807.

[97] J. Nylk, K. McCluskey, S. Aggarwal, J. A. Tello, K. Dholakia, Enhancement of image quality and imaging depth with airy light-sheet microscopy in cleared and non-cleared neural tissue, Biomedical Optics Express 7 (2016) 4021–4033.

[98] J. Nylk, K. McCluskey, M. A. Preciado, M. Mazilu, Z. Yang, F. J. Gunn-Moore, S. Aggarwal, J. A. Tello, D. E. Ferrier, K. Dholakia, Light-sheet microscopy with attenuation-compensated propagation-invariant beams, Science Advances 4 (2018) eaar4817.

[99] J. Swoger, M. Muzzopappa, H. López-Schier, J. Sharpe, 4d retrospective lineage tracing using spim for zebrafish organogenesis studies, Journal of Biophotonics 4 (2011) 122–134.

[100] J. Icha, C. Kunath, M. Rocha-Martins, C. Norden, Independent modes of ganglion cell translocation ensure correct lamination of the zebrafish retina, J Cell Biol 215 (2016) 259–275.

[101] Y. Xiao, A. Faucherre, L. Pola-Morell, J. M. Heddleston, T.-L. Liu, T.-L. Chew, F. Sato, A. Sehara-Fujisawa, K. Kawakami, H. López-Schier, High-resolution live imaging reveals axon-glia interactions during peripheral nerve injury and repair in zebrafish, Disease models & mechanisms 8 (2015) 553–564.

[102] E. J. Gualda, D. Simão, C. Pinto, P. M. Alves, C. Brito, Imaging of human differentiated 3d neural aggregates using light sheet fluorescence microscopy, Frontiers in Cellular Neuroscience 8 (2014) 221.

[103] N. Vladimirov, Y. Mu, T. Kawashima, D. V. Bennett, C.-T. Yang, L. L. Looger, P. J. Keller, J. Freeman, M. B. Ahrens, Light-sheet functional imaging in fictively behaving zebrafish, Nature Methods 11 (2014) 883.

[104] S. Wolf, W. Supatto, G. Debrégeas, P. Mahou, S. G. Kruglik, J.-M. Sintes, E. Beaurepaire, R. Candelier, Whole-brain functional imaging with two-photon light-sheet microscopy, Nature Methods 12 (2015) 379.

[105] W. C. Lemon, S. R. Pulver, B. Höckendorf, K. McDole, K. Branson, J. Freeman, P. J. Keller, Whole-central nervous system functional imaging in larval drosophila, Nature Communications 6 (2015) 7924.

[106] P. Haslehurst, Z. Yang, K. Dholakia, N. Emptage, Fast volume-scanning light sheet microscopy reveals transient neuronal events, Biomed. Opt. Express 9 (2018) 2154–2167.

[107] A. Ertürk, K. Becker, N. Jährling, C. P. Mauch, C. D. Hojer, J. G. Egen, F. Hellal, F. Bradke, M. Sheng, H.-U. Dodt, Three-dimensional imaging of solvent-cleared organs using 3disco, Nature Protocols 7 (2012) 1983.

[108] K. Becker, N. Jährling, S. Saghafi, R. Weiler, H.-U. Dodt, Chemical clearing and dehydration of gfp expressing mouse brains, PloS one 7 (2012) e33916.

[109] T. Kuwajima, A. A. Sitko, P. Bhansali, C. Jurgens, W. Guido, C. Mason, Cleart: a detergent-and solvent-free clearing method for neuronal and non-neuronal tissue, Development 140 (2013) 1364–1368.

[110] M.-T. Ke, S. Fujimoto, T. Imai, Seedb: a simple and morphology-preserving optical clearing agent for neuronal circuit reconstruction, Nature Neuroscience 16 (2013) 1154.

[111] K. Chung, J. Wallace, S.-Y. Kim, S. Kalyanasundaram, A. S. Andalman, T. J. Davidson, J. J. Mirzabekov, K. A. Zalocusky, J. Mattis, A. K. Denisin, et al., Structural and molecular interrogation of intact biological systems, Nature 497 (2013) 332.

[112] N. Renier, Z. Wu, D. J. Simon, J. Yang, P. Ariel, M. Tessier-Lavigne, idisco: a simple, rapid method to immunolabel large tissue samples for volume imaging, Cell 159 (2014) 896–910.

[113] R. Tomer, L. Ye, B. Hsueh, K. Deisseroth, Advanced clarity for rapid and high-resolution imaging of intact tissues, Nature Protocols 9 (2014) 1682.

[114] M. K. Schwarz, A. Scherbarth, R. Sprengel, J. Engelhardt, P. Theer, G. Giese, Fluorescent-protein stabilization and high-resolution imaging of cleared, intact mouse brains, PLoS One 10 (2015) e0124650.

[115] M. Stefaniuk, E. J. Gualda, M. Pawlowska, D. Legutko, P. Matryba, P. Koza, W. Konopka, D. Owczarek, M. Wawrzyniak, P. Loza-Alvarez, et al., Light-sheet microscopy imaging of a whole cleared rat brain with thy1-gfp transgene, Scientific Reports 6 (2016) srep28209.

[116] C. Pan, R. Cai, F. P. Quacquarelli, A. Ghasemigharagoz, A. Lourbopoulos, P. Matryba, N. Plesnila, M. Dichgans, F. Hellal, A. Ertürk, Shrinkage-mediated imaging of entire organs and organisms using udisco, Nature Methods 13 (2016) 859–867.

[117] E. Lugo-Hernandez, A. Squire, N. Hagemann, A. Brenzel, M. Sardari, J. Schlechter, E. H. Sanchez-Mendoza, M. Gunzer, A. Faissner, D. M. Hermann, 3d visualization and quantification of microvessels in the whole ischemic mouse brain using solvent-based clearing and light sheet microscopy, Journal of Cerebral Blood Flow & Metabolism 37 (2017) 3355–3367.

[118] A. P. Di Giovanna, A. Tibo, L. Silvestri, M. C. Müllenbroich, I. Costantini, L. Sacconi, P. Frasconi, F. S. Pavone, Optimal staining and clearing protocol for whole mouse brain vasculature imaging with light-sheet microscopy, in: European Conference on Biomedical Optics, Optical Society of America, 2017, p. 104140N.

[119] M. Plöschner, V. Kollárová, Z. Dostál, J. Nylk, T. Barton-Owen, D. E. Ferrier, R. Chmelík, K. Dholakia, T. Čižmár, Multimode fibre: Light-sheet microscopy at the tip of a needle, Scientific Reports 5 (2015) 18050.

[120] C. J. Engelbrecht, F. Voigt, F. Helmchen, Miniaturized selective plane illumination microscopy for high-contrast in vivo fluorescence imaging, Optics Letters 35 (2010) 1413–1415.

[121] L. A. Royer, W. C. Lemon, R. K. Chhetri, Y. Wan, M. Coleman, E. W. Myers, P. J. Keller, Adaptive light-sheet microscopy for long-term, high-resolution imaging in living organisms, Nature Biotechnology 34 (2016) 1267.

[122] P. J. Keller, M. B. Ahrens, Visualizing whole-brain activity and development at the single-cell level using light-sheet microscopy, Neuron 85 (2015) 462–483.

Highligths:

- LSFM is increasingly becoming an interesting technique for neuroimaging.
- LSFM opened up the possibility of imaging in vivo the development of the CNS.
- LSFM allows acquiring morphological images of whole cleared mammalian brains with sub-cellular resolution.
- The use of propagation invariant beams has shown potential for imaging in turbid neural tissues.
- Single objective LSFM implementations and fibre based LSFM could allow in depth in vivo imaging.